http://dx.doi.org/10.5012/bkcs.2012.33.2.657

Biological Toxicity Changes of Mercaptoacetic Acid and Mercaptopropionic Acid Upon Coordination onto ZnS:Mn Nanocrystal

Hoon Young Kong, Cheong-Soo Hwang,† and Jonghoe Byun*

*Department of Molecular Biology and †Department of Chemistry and, Institute of Nanosensor and Biotechnology, Dankook University, Gyeonggi-do 448-701, Korea. *E-mail: jonghoe@dankook.ac.kr*
Received November 23, 2011, Accepted January 30, 2012

Mercaptoacetic acid (MAA) and mercaptopropionic acid (MPA) capped ZnS:Mn nanocrystals were synthesized and their physical characteristics were examined by XRD, HR-TEM, EDXS, and FT-IR spectroscopy. The optical properties of the MPA capped ZnS:Mn nanocrystals dispersed in aqueous solution were also measured by UV/Vis and solution photoluminescence (PL) spectra, which showed a broad emission peak around 598 nm (orange light emissions) with calculated relative PL efficiency of 5.2%. Comparative toxicity evaluation of the uncoordinated ligands, MAA and MPA, with the corresponding ZnS:Mn nanocrystals revealed that the original ligands significantly suppressed the growth of wild type *E. coli* whereas the ligand-capped nanocrystals did not show significant toxic effects. The reduced cytotoxicity of the conjugated ZnS:Mn nanocrystals was also observed in NIH/3T3 mouse embryonic fibroblasts. These results imply that potential toxicities of the capping ligands can be neutralized on ZnS:Mn surface.

Key Words : ZnS:Mn nanocrystal, MAA and MPA capping, Toxicity, *E. coli*, NIH/3T3

Introduction

Low dimensional semiconductor nanocrystals have gained a lot of attention due to their size-dependent physical properties and wide application in electronic devices and biological sensors.[1,2] There have been many efforts to develop quantum dots having higher quantum efficiencies, more accessible light absorption wavelengths, and narrower emission bands.[3-5] Incorporation of transition metal ions into semiconductor nanocrystals can cause radiative recombination of excited electron-hole pair at the dopant ion sites rather than at surfaces, which could shift photoluminescence wavelength and increase quantum efficiency.[6,7] Therefore, transition metal ion-doped semiconductor nanocrystals hold great potential for applications in the fields such as display, LED devices, and imaging. One of the representative examples of metal ion-doped nanocrystals would be an orange-light emitting manganese-ion doped ZnS nanocrystallite (ZnS:Mn) that exhibits both high photoluminescent efficiency and thermal stability at ambient temperature.[8] These advantages of ZnS:Mn make it an attractive alternative to organic dyes, which can be used as fluorescent probes in biological system.

Recently, a lot of progress has been made in the developments of preparation methods for nanocrystals. The synthetic routes include the use of gas, solid, and aqueous solution reactions *via* organometallic precursors. Unfortunately, however, these methods often require very high temperatures, pressures and even the use of extremely hazardous chemicals that may not be compatible with living cell.[9] For these nanocrystals to have biological application, it is therefore critically important to reduce potential toxicities of nanocrystals. In this regard, functionalization of nanocrystal surface with biocompatible surfactants is an important issue in nanocrystal fabrications.[10] In particular, it is crucial to make nanoparticles water-dispersible for many biological applications. In many cases, surfactants play an important role in the control of particle sizes, optical properties, and solubility of nanocrystals in certain solvents.[11] Most common synthetic scheme for water-dispersible nanocrystals have used polar surface capping ligands, such as mercaptoacetate (MAA) and sulfodiisooctyl succinate (AOT) molecules, to form a micelle structure with negative charges evenly distributed on its surface. In addition, it has been shown that the photoluminescence efficiency for AOT capped ZnS:Mn nanocrystals increases several fold after surface modification.[12] Previously, synthesis and spectroscopic characterization of water-dispersible manganese-ion doped ZnS nanoparticles that are stabilized by mercaptoacetic acid (ZnS:Mn-MAA) was reported together with their DFT calculations.[13] In the present study, we report on the synthesis of two similar manganese-ion doped ZnS nanoparticles that are stabilized by mercaptoacetic acid and mercaptopropionic acid molecules (ZnS:Mn-MAA and ZnS:Mn-MPA, respectively). Secondly, potential biological toxicities of ZnS:Mn-MAA and ZnS:Mn-MPA are compared with the uncoordinated original MAA and MPA molecules in typical bacteria and animal cells.

Experimental Section

Instrumentation. UV/vis absorption spectra were recorded using a Perkin Elmer Lambda 25 spectrophotometer equipped with a deuterium/tungsten lamp. The FT-IR spectra were obtained using a Perkin Elmer spectrophotometer equipped an attenuated total reflection (ATR) unit. Solution

photoluminescence spectra were taken by a Perkin Elmer LS-45 spectrophotometer equipped with a 500 W Xenon lamp, 0.275 m triple grating monochromator, and PHV 400 photomultiplier tube. HR-TEM images were taken with a JEOL JEM 1210 electron microscope with a MAG mode of 1,000 to 800,000. The accelerating voltage was 40-120 kV. Samples for TEM were prepared *via* dispersion in methanol and placement on a carbon-coated copper grid (300 Mesh) followed by drying under vacuum. In addition, elemental compositions of the nanocrystals were determined by an Energy Dispersive X-ray Spectroscopy (EDXS) collecting unit equipped in the HR-TEM, with a Si (Li) detector in IXRF 500 system. ICP-AES elemental analysis for the ZnS:Mn-MAA and ZnS:Mn-MPA nanocrystals were performed by Optima-430 (Perkin Elmer) spectrometer equipped with Echelle optics system and Segmented array charge coupled device (SCD) detector. To prepare a sample of corresponding nanocrystal, a 0.5 mL of the concentrated nanocrystal solution was mixed with 9.5 mL of concentrated nitric acid over the period of 3 days. After which 0.5 mL of the digested solution is placed in a 9.5 mL of nanopure-water.

Chemicals and Reagents. All solvents, except deionized water, were purchased from Aldrich (reagent grade) and distilled prior to use. All reactants, including mercaptoacetic acid (MAA), mercaptopropionic acid (MPA), $ZnSO_4$, $MnSO_4$, and Na_2S, were purchased from Aldrich and used as received. The *E. coli* K-12 (wild type strain) was purchased from the Korean Culture Center of Microorganisms (KCCM 40939). Etoposide was purchased form Sigma Aldrich (reagent grade). NIH/3T3 was purchased from American Type Culture Collection (CRL-1658) and Dulbecco's Modified Eagle Medium (DMEM) and fetal bovine serum were purchased from Gibco (11965118 and 10099141).

Synthesis of MAA and MPA Capped ZnS:Mn Nanocrystals. A previously reported aqueous synthesis of MAA and MPA capped ZnS:Mn nanocrystals *via* the formation of zinc (II) ion containing complexes as reactive intermediates was followed with slight modification.[13] A 50 mL aqueous solution of $ZnSO_4 \cdot 5H_2O$ (1.44 g, 5 mmol) was slowly added to a 50 mL aqueous solution containing 10 mmol of MAA or MPA and NaOH (0.40 g, 10 mmol) at 5 °C (ice-water bath). The solution was warmed to ambient temperature after 1 hour's stirring. Separate from this, $MnSO_4 \cdot H_2O$ (0.02 g, 0.1 mmol) and Na_2S (0.40 g, 5 mmol) were dissolved in 20 mL 0.01 M HCl. This mixture was subsequently transferred to the flask containing the Zn-MAA or the Zn-MPA complexes under vigorous stirring. The resulting solution was refluxed for 10 hours. Slow cooling to ambient temperature and the addition of ethanol resulted in a yellow-white precipitate at the bottom of the flask. Finally, the obtained solids were separated by centrifuging and decanting the supernatant. The solids were then dried for 24 hours in a vacuum oven. The experimental data are summarized in Table 1.

Table 1. Data Summary for the MAA and MPA capped ZnS:Mn nanocrystals

	ZnS:Mn (MAA) Ref.13	ZnS:Mn (MPA)
UV/vis (λ_{max}, nm)	307	320
PL emission wavelength (λ_{max}, nm)	575	598
PL efficiency (%)	4.8	5.2
Mn doping (%)	1.7	2.56
Particle sizes by TEM (nm)	3.8	5.0
FT-IR ν (cm^{-1})	2951(s), 2912(w) 1597(s), 1398(s) 1170(w), 932(m) 787(s), 585(w) 502(m), 259(s)	3190(s), 2185(w) 1985(w), 1641(w) 1548(s), 1391(s) 1296(w), 1265(w) 1106(w), 1009(s)

Toxicity Tests in Bacteria. *E. coli* K-12 strain was grown in 5 mL of nutrient broth (beef extract 3 g/L, peptone 5 g/L, NaCl 10 g/L) with shaking at 37 °C for 16 hrs. MPA was added to 5 mL of nutrient broth to give a final concentration of 57 μM at 37 °C and this stock solution was used to achieve 2-fold serial dilutions (5.7 to 0.7 μM). MAA was added to 5 mL of nutrient broth to give a concentration of 72 μM at 37 °C and this stock solution was used to achieve different concentrations (0.14, 0.72, 1.4 and 7.2 μM). The nanocrystals (ZnS:Mn-MAA or ZnS:Mn-MPA) were dissolved in 5 mL of the nutrient broth at 37 °C to give a final concentration of 10 mg/mL and this stock solution was used to achieve different concentrations in 18 mL bacterial culture (0 to 1 mg/mL). After making each nutrient broth containing different amount of MAA, MPA, or quantum dots, the *E. coli* K-12 that had been grown overnight (16 hr) was inoculated to the nutrient broth. To plot growth curve, the turbidity of the culture was examined every 30 min by measuring optical density at 600 nm using SpectraMax M2e microplate reader (Molecular Devices). The study was performed in triplicates.

Toxicity Tests in Animal Cells. Mouse embryonic fibroblast cells (NIH/3T3) were cultured at 37 °C under humidified atmosphere (5% CO_2) in Dulbecco's Modified Eagle Medium (DMEM) containing 10% (v/v) fetal bovine serum. For real-time cell toxicity assay, an impedance-based real-time cell analyzer (RTCA, xCELLigence, Roche) was used. Briefly, to obtain background readout, NIH3T3 cells (9×10^3/50 μL) were added to each well of E-plate 16. After cell seeding, E-plate 16 was incubated at room temperature for 30 min before installation onto RTCA-DP instrument. Then the instrument was incubated at 37 °C in humidified atmosphere of 5% CO_2. One day later, the cells were treated with ZnS:Mn-MAA or ZnS:Mn-MPA and monitored every 10 minutes for change in cell index. The detailed principles of xCELLigence real-time cell analyzer technology have been described previously.[14,15]

Statistical Analysis. The data were expressed as means ± SD. Results were analyzed with GraphPad Prism statistics software (GraphPad Software, Inc., La Jolla, CA, USA). Student's *t*-test was used to evaluate statistical differences between the groups. A *P* value less than 0.05 was considered statistically significant.

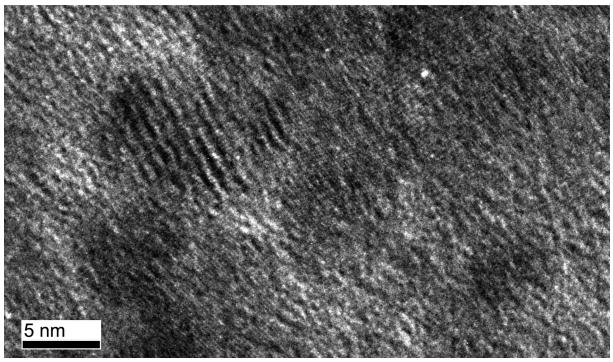

Figure 1. HR-TEM image of ZnS:Mn-MPA.

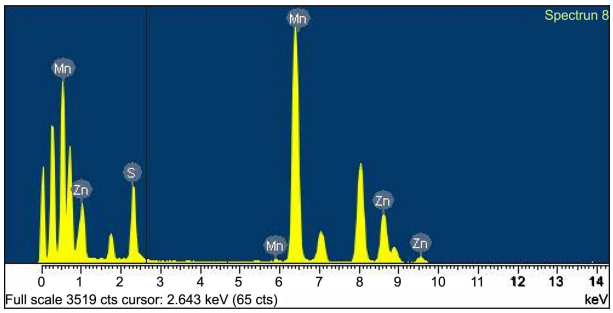

Figure 2. Energy dispersive x-ray spectroscopy (EDXS) diagram of ZnS:Mn-MPA.

Results and Discussions

This study evaluates the toxicity profiles of water-dispersible ZnS:Mn nanocrystals whose surfaces had been modified with the mercaptoacetic acid (MAA) and mercaptopropionic acid (MPA). Prior to biological evaluation, the physical and optical characteristics of the nanocrystals were examined and experimental data for the ZnS:Mn-MAA were reconfirmed. The particle sizes of the MPA capped ZnS:Mn nanocrystals were measured from the HR-TEM images (Figure 1). The images show fairly homogeneous spherical 5.2 nm diameter particles on average.

Figure 2 presents a result of energy dispersive X-ray spectroscopy (EDXS) elemental analysis of the solid product of the ZnS:Mn-MPA. The presence of zinc, sulfur and manganese were confirmed besides the large amounts of carbon and oxygen atoms in the powder samples, which were not assigned in the diagram. In addition, EDXS analysis showed that the doping percentages of the manganese ions in the measured ZnS:Mn nanoparticles were 2.56% for the ZnS:Mn-MPA nanocrystal. The manganese (II) ion doping concentration in the ZnS:Mn crystals was designed to be approximately 2.0%, a previously reported optimum of PL efficiency for other ligand-capped ZnS:Mn nanocrystals.[16]

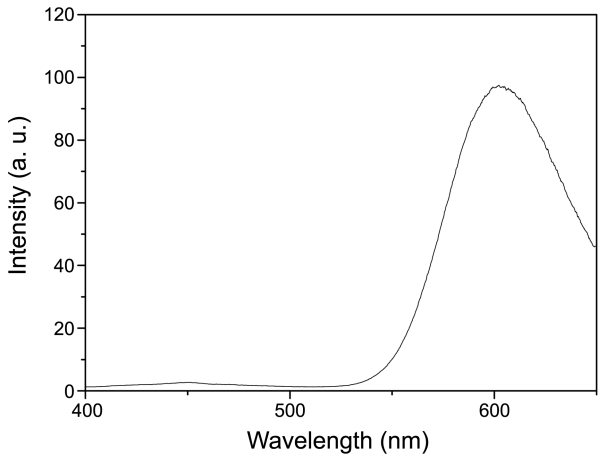

Figure 3. Room temperature aqueous solution photoluminescence emission spectrum of ZnS:Mn-MPA.

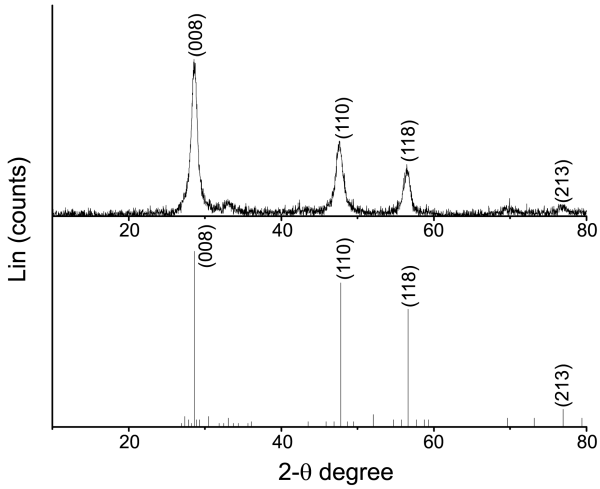

Figure 4. XRD diagram of ZnS:Mn-MPA nanocrystal. The lower panel shows the XRD spectrum of bulk ZnS in a hexagonal wurtzite form.

Optical properties of the ZnS:Mn-MPA were measured *via* room temperature solution photoluminescence (PL) spectroscopy, as shown in Figure 3. The solution PL spectra, obtained from the MPA-capped ZnS:Mn in aqueous solution, showed broad emission peaks appeared at 598 nm. The presented emission spectrum was obtained when the excitation wave length was fixed at UV/vis absorption peak of 320 nm (Table 1). The observed large Stokes shift for the MPA-capped ZnS:Mn nanocrystal is typical of nano-sized crystalline materials.[17] The PL efficiency of the ZnS:Mn-MPA nanocrystal was measured and calculated using the method reported by Williams *et al.*[18] This method involves calculating the relative quantum yield through a comparison with a standard material, 0.1 M aqueous solution of L-Tyrosine, whose excitation wavelength and absolute quantum yield were respectively reported to be 275 nm and 14% (at 22 °C). The obtained relative PL efficiency of the ZnS:Mn nanocrystal was 5.2%.

The wide angle X-ray diffraction patterns of powder sample of the MPA-capped ZnS:Mn nanocrystal was obtained (Figure 4). Most of the peaks are broad; however, they are quite common features of most low-dimensional nano-sized materials.[19] Even so, there were clearly indexable (008), (110) and (118) peaks in the spectra indicating that all the amino acids-capped ZnS:Mn nanocrystals are in hexagonal wurtzite phases in the space group of $P6_3mc$.[20]

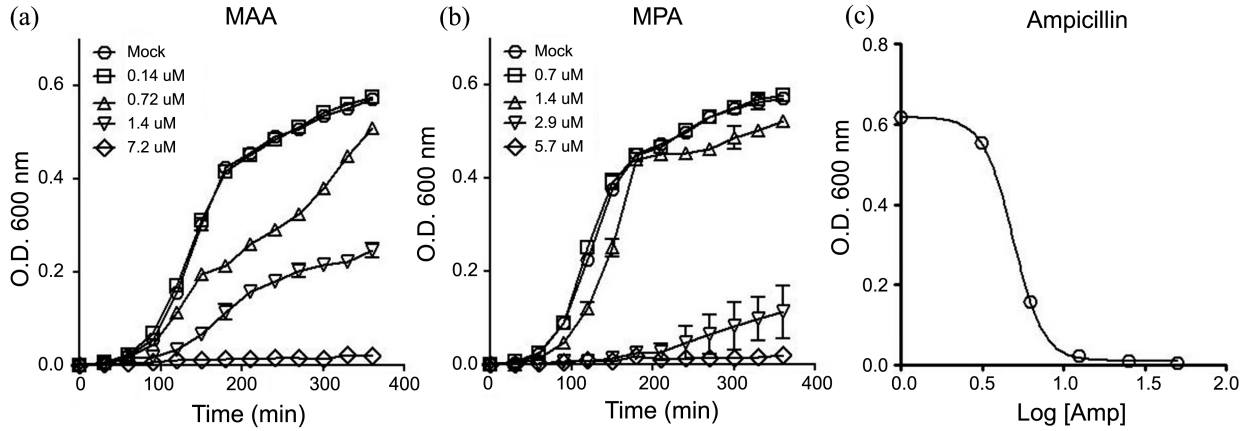

Figure 5. Effect of MAA (a) and MPA (b) on the growth of *E. coli* K-12 strain. Estimation of IC_{50} for antibiotic, Ampicillin, in the same bacteria (c).

In addition, the MPA molecules on the surfaces of the ZnS:Mn nanocrystals were characterized by FT-IR spectroscopy. All obtained peak data are listed in Table 1. The peaks that appeared near 2185 cm^{-1} and 1548 cm^{-1} were assigned as zinc coordinated -SH and $-COO^-$ groups of the MPA molecule.[21] To remove any uncoordinated or unreacted MPA molecules, the centrifuged white solids were rapidly washed several times with cold alcohol/water solutions. As a result, the peaks that resulted from the precursors, free MPA molecules, could be removed from the presented FT-IR data.

Since MPA- and MAA-capped water-soluble ZnS:Mn semiconductor nanocrystals were successfully synthesized, we examined potential toxicities of MPA- and MAA-capped water-soluble ZnS:Mn semiconductor nanocrystals together with their uncoordinated MAA and MPA ligands in typical enteric bacteria (*Escherichia coli* K-12). By monitoring the growth curve of *E. coli* in the presence and absence of test molecules, any toxic effects could be easily identified. As shown in Figure 5, both MAA and MPA had toxic effects on the growth of *E. coli* in a concentration-dependent manner. When the two reagents were compared at the same 1.4 μM concentration, greater inhibition was seen in MAA group than in MPA group. Similar trend was observed near 0.7 μM concentrations. To confirm that the bacteria used in this study are also inhibited by antibiotic, different concentrations of ampicillin was used for growth inhibition and the concentrations that result in 50% bacterial inhibition (IC_{50}) was determined at 4.91 μg/mL (Figure 5(c)).

However, different results were obtained with the ZnS:Mn nanocrystals capped with MAA or MPA (Figure 6). Unlike the free MAA or MPA, these conjugated nanocrystals had little toxicities as indicated by little difference in growth kinetics from the mock group. This compelling observation strongly suggests the safety of MAA and MPA capped ZnS:Mn nanocrystals and their potential application as biocompatible water-dispersible quantum dots. Interestingly, at the highest concentration (1 mg/mL), both ZnS:Mn-MAA and ZnS:Mn-MPA groups showed aberrant growth curves, which is indicative of artifacts that may have been caused by experimental conditions. Next, based on optical density (600 nm) data at 6 hr, we calculated IC_{50} values using GraphPad Prism 5 software (La Jolla, CA, USA). The obtained IC_{50} values for uncoordinated MAA and MPA were; [MAA] = 1.26×10^{-6} M and free [MPA] = 2.14×10^{-6} M, while that for the nanocrystal coordinated ZnS:Mn-MAA and ZnS:Mn-MPA were ^{MAA}[ZnS:Mn] = 6.24×10^{-5} M and ^{MPA}[ZnS:Mn] = 3.36×10^{-5} M, respectively. The concentrations of the nanocrystals in aqueous solution, represented as [ZnS:Mn], were determined by elemental analysis by ICP-AES measurements as described in the literature.[22] The obtained Zn

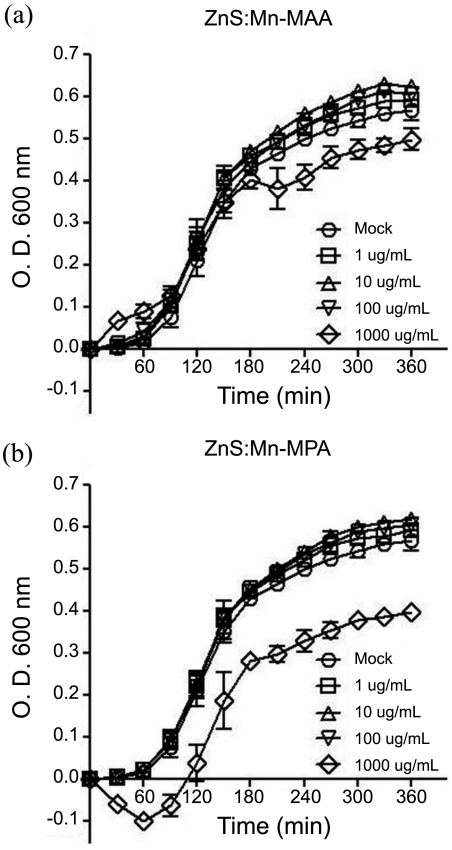

Figure 6. Effect of MAA (a) and MPA (b) capped ZnS:Mn nanocrystals on the growth of *E. coli* K-12 strain.

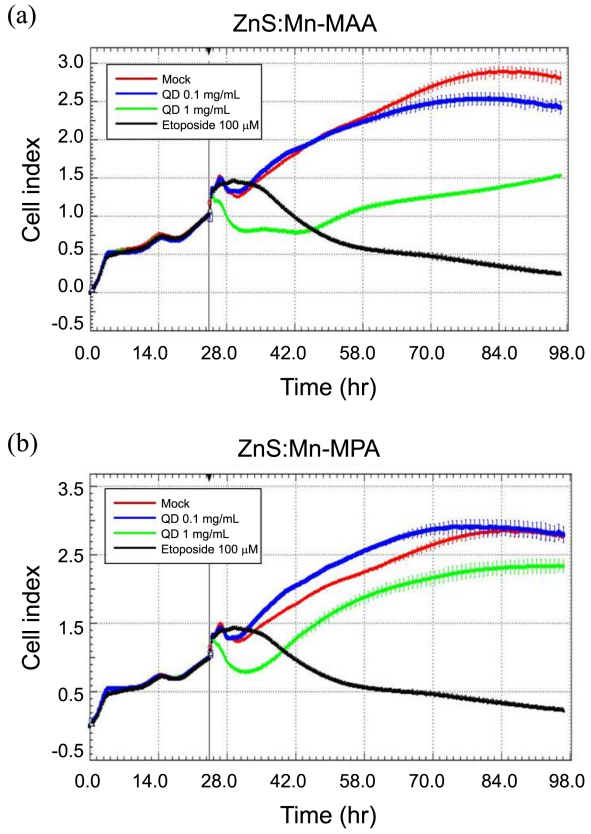

Figure 7. Real-time cellular toxicity assay of MAA (a) and MPA (b) capped ZnS:Mn nanocrystals in NIH/3T3 cells. The xCELLigence System (RTCA-DP) monitors cellular events in real time without the incorporation of labels. The System measures electrical impedance across interdigitated micro-electrodes integrated on the bottom of tissue culture E-Plates. The impedance measurement provides quantitative information about the biological status of the cells including cell number and viability. Mock and 100 μM etoposide-treated groups served as negative and positive controls, respectively.

and Mn concentrations were combined and converted into the nanocrystal particle concentration, assuming that the nanocrystal particle holds the same density as its bulk material. For both molecules, the obtained IC_{50} values revealed that their biological toxicities seemed to be reduced about fifteen to fifty fold after coordination to the ZnS:Mn nanocrystals. Moreover, among the uncoordinated free molecules, MPA showed less toxicity than MAA in some extent; however, after coordination to the surface of the ZnS:Mn nanocrystals, the biological toxicities were inversed so that the ZnS:Mn-MPA appeared to be more toxic on the growth of *E. coli*. It is hard to conclude that the toxic nature of the corresponding molecules were changed during the coordination to the ZnS:Mn nanocrystals, but probably it is more closely related to their capping abilities on the ZnS:Mn nanocrystal surfaces. The MPA molecule contains extra terminal methyl group which is freely rotating in solution state to create more bulkiness than MAA; therefore, one can expect that the capping layer formed by the MPA molecules on the surface of the ZnS:Mn nanocrystal has more rooms for the zinc atoms in the nanocrystal to be dissociated from the surface to release Zn^{2+} ions, which is also known as a major cause of the biological toxicity by the most nanosized inorganic semiconductor materials.[23]

Next, we evaluated potential toxicity of MAA and MPA capped ZnS:Mn nanocrystals in NIH/3T3, a typical mammalian fibroblast cell line. To monitor cytotoxicity in real-time, xCELLigence real time cell analyzer (RTCA) that does not use any labels were employed (Figure 7). This label-free device measures electrical impedance, which is displayed as cell index (CI) value, across interdigitated micro-electrodes integrated on the bottom of tissue culture E-Plates. The CI measurement provides quantitative information about the biological status of the cells such as cell number and viability.[14,15] The presence of the cells on top of the electrodes affects the local ionic environment at the electrode/solution interface and leads to an increase in the CI value. Thus, CI is a quantitative measure of cell number present in a well. As shown in Figure 7, both groups had CI values lower than Mock group at 1 mg/mL dose, suggesting potential cytotoxicity in NIH/3T3 cells. But MPA capped ZnS:Mn group had higher CI values than MAA capped ZnS:Mn group, which is consistent with free MPA and MAA data in bacteria (Figure 5). In other aspect, both MPA and MAA capped ZnS:Mn groups showed recovery of CI over time. These recovery curves contrast with that of etoposide (apoptosis-inducing agent)-treated group which showed continued decrease in CI value. This observation implies that the cellular damages caused by these nanocrystals may be transient and can be overcome through time. At 0.1 mg/mL dose, little toxicities were found in both groups suggesting that capping ZnS:Mn with MAA or MPA may be a viable approach for biological applications.

The biological toxicity tests for the nanocrystals were performed in the concentration range of 4.8×10^{-7} M to 4.8×10^{-4} M for ZnS:Mn-MAA, and 7.4×10^{-7} M to 7.4×10^{-4} M for ZnS:Mn-MPA, respectively, which corresponds to the concentration range from 1 ug/mL to 1 mg/mL for both nanocrystal solid samples used as presented in Figures 6 and 7. Dua *et al*. have reported similar biological toxicity test of CdSe and CdSe/ZnS quantum dots in *E. coli* and HEK293 cells.[24] They found that overall toxicity of CdSe was reduced after shell capping by ZnS nanocrystal layer. For instance, in their experiments, obtained IC_{50} value for Green light emitting CdSe nanocrystal was 8.35 nM after 24 hour exposure to the test cells, while that for the CdSe/ZnS core-shell quantum dot was 135.98 nM. As a result, the biological toxicity for the CdSe nanocrystal was significantly reduced by simply capping the surface by ZnS, an inorganic nanocrystal lattice layer. In their experiment, the reported test concentration range for the CdSe and CdSe/ZnS nanocrystals were from 10 nM to 200 nM.

The present finding that toxic capping materials such as MAA and MPA can be made harmless by conjugating into ZnS:Mn nanocrystal is intriguing. This is more significant when we consider the fact that both MAA and MPA are among the most commonly used polar surface capping ligands for water-dispersible nanocrystals. Other nanocrystals

such as CdSe/ZnSe capped with MPA had little toxicity compared with negative control group and lower toxicity than the CdSe/ZnSe capped with GA/TOPO.[25] In addition, CdSe quantum dots capped with MAA had the better stability than the CdSe capped with Cys, both in terms of photostability and heat-stability, leading to less toxicity.[26,27] These results are consistent with the present finding that MAA or MPA, which are toxic to the cells, can be rendered less toxic through surface capping onto nanocrystals. It can be speculated that the functional groups of MPA or MAA molecules which are involved in biological toxicity are masked by binding to metal and/or non-metal parts of the nanocrystals. Detailed mechanistic analysis of these aspects needs further study.

Our study strongly suggests that careful combination of capping materials with ZnS:Mn nanocrystals can help us to overcome the potential toxicity problems of quantum dots. More study is warranted to determine the factors governing cytotoxicity of capping materials as well as nanocrystals, including the degree and stability of surface capping, chemical composition, size, shape and surface charge.[25]

Conclusion

In summary, Mercaptoacetic acid (MAA) and Mercaptopropionic acid (MPA)-capped water-dispersible ZnS:Mn nanocrystals (ZnS:Mn-MAA and ZnS:Mn-MPA) were successfully made and their biological effects on enteric bacteria and animal cells were investigated. Comparative studies of toxicities of uncoordinated ligands, MAA and MPA, with those of the corresponding nanocrystals revealed that original ligands significantly suppressed the growth of wild type *E. coli* K-12 strain whereas the nanocrystals capped with those ligands did not show significant toxic effects. The reduced cytotoxicity of the conjugated nanocrystals was also observed in NIH/3T3 mouse embryonic fibroblasts, strongly suggesting that the water-dispersible MAA and MPA capped ZnS:Mn nanocrystals have safe physico-chemical properties suitable for biological applications.

Recently, semiconductor quantum dots (QDs) have received much attention as a novel type of fluorophore for biomedical imaging. Since MAA or MPA capping of the water-dispersible ZnS:Mn semiconductor nanocrystals can provide a novel platform on which many biomolecules such as DNA, RNA, and proteins can be attached, the present finding that the toxicity of MAA and MPA can be reduced through conjugation bears big significance. The water-dispersible MAA and MPA capped ZnS:Mn nanocrystals should find wide application in diverse biomedical fields, including biosensors and molecular imaging.

Acknowledgments. The present research was conducted by the research fund of Dankook University in 2009.

References

1. Alivisatos, A. P. *J. Phys. Chem.* **1996**, *100*, 13226.
2. Murray, C. B.; Kagan, C. R.; Bawendi, M. G. *Annu. Rev. Mater. Sci.* **2000**, *30*, 545.
3. Bhargava, R. N.; Gallagher, D.; Hong, X.; Nurmikko, *A. Phys. Rev. Lett.* **1994**, *72*, 416.
4. Gan, L. M.; Liu, B.; Chew, C. H.; Xu, S. J.; Chua, S. J.; Loy, G. L.; Xu, G. Q. *Langmuir* **1997**, *13*, 6427.
5. Bol, A. A.; Meijerink, A. *Phys. Rev. B: Condens. Matter* **1998**, *58*, R15997.
6. Xu, S. J.; Chua, S. J.; Liu, B.; Gan, L. M.; Chew, C. H.; Xu, G. Q. *Appl. Phys. Lett.* **1998**, *73*, 478.
7. Tanaka, M.; Sawai, S.; Sengoku, M.; Kato, M.; Masumoto, Y. *J. Appl. Phys.* **2000**, *87*, 8535.
8. Hwang, J. M.; Oh, M. O.; Kim, I.; Lee, J. K.; Ha, C. S. *Curr. Appl. Phys.* **2005**, *5*, 31.
9. Yu, S. H.; Wu, Y. S.; Yang, J.; Han, Z.; Xie, Y.; Qian, Y.; Liu, X. *Chem. Mater.* **1998**, *10*, 2309.
10. Jun, Y. W.; Jang, J. T.; Cheon, J. W. *Bull. Korean Chem. Soc.* **2006**, *27*, 961.
11. Chan, W. C. W.; Nie, S. *Science* **1998**, *281*, 2016.
12. Chen, C. C.; Yet, C. P.; Wang, H. N.; Chao, C. Y. *Langmuir.* **1999**, *15*, 6845.
13. Kim, J. E.; Hwang, C. S.; Yoon, S. *Bull. Kor. Chem. Soc.* **2008**, *29*, 1247.
14. Abassi, Y. A.; Jackson, J. A.; Zhu, J.; O'Connell, J.; Wang, X.; Xu, X. *J. Immunol Methods* **2004**, *292*, 195.
15. Xing, J. Z.; Zhu, L.; Jackson, J. A.; Gabos, S.; Sun, X. J.; Wang, X. B.; Xu, X. *Chem. Res. Toxicol.* **2005**, *18*, 154.
16. Yi. G.; Sun, B.; Yang, F.; Chen, D. *J. Mater. Chem.* **2001**, *11*, 2928.
17. Bhargava, R. N.; Gallagher, D.; Hong, X.; Nurmikko, A. *Phys. Rev. Lett.* **1994**, *72*, 416.
18. Williams, A. T. R.; Winfield, S. A.; Miller, J. N. *Analyst* **1983**, *108*, 1067.
19. Brus, L. E. *Appl. Phys. A* **1991**, *53*, 465.
20. Zhuang, J.; Zhang, X.; Wang, G.; Li, D.; Yang, W.; Li, T. *J. Mater. Chem.* **2003**, *13*, 1853.
21. Moszczenski, C. W.; Hooper, R. J. *Inorg. Chim. Acta.* **1983**, *70*, 71.
22. Yu, W. W.; Qu, L.; Guo, W.; Peng, X. *Chem. Mater.* **2003**, *15*, 2854.
23. Hardman, R. *Environ. Health Perspect*. **2006**, *114*, 165.
24. Dua, P.; Jeong, S.; Lee, S. E.; Hong, S. W.; Kim, S.; Lee, D.-K. *Bull. Kor. Chem. Soc*. **2010**, *31*, 1555.
25. Mahto, S. K.; Park, C.; Yoon, T. H.; Rhee, S. W. *Toxicol. In Vitro* **2010**, *24*, 1070.
26. Wang, L.; Zheng, H.; Long, Y.; Gao, M.; Hao, J.; Du, J.; Mao, X.; Zhou, D. *J. Hazard Mater.* **2010**, *177*, 1134.
27. Zhang, Y. H.; Zhang, H. S.; Ma, M.; Guo, X. F.; Wang, H. *Appl. Surf. Sci.* **2009**, *255*, 4747.